Molecular Therapy
Nucleic Acids
Original Article

A CRISPR-Cas9 library screening identifies CARM1 as a critical inhibitor of ferroptosis in hepatocellular carcinoma cells

Yiming Cheng,[1,5] Xiaochen Wang,[1,5] Shuyu Huang,[1] Liang Zhang,[2] Bei Lan,[1] Xuanyuan Li,[1] Hao Chen,[1] Zhenfeng Liu,[1] Yijie Su,[1] Lishan Xi,[1] Shengyun Feng,[1] Yanxuan Guo,[1] Jun Zhou,[3] Yingmei Wang,[4] and Chenghao Xuan[1]

[1]Tianjin Key Laboratory of Female Reproductive Health and Eugenetics, Tianjin Medical University General Hospital, The Province and Ministry Co-sponsored Collaborative Innovation Center for Medical Epigenetics, Department of Biochemistry and Molecular Biology, Tianjin Medical University, Tianjin 300070, China; [2]Research Center of Translational Medicine, Jinan Central Hospital Affiliated to Shandong First Medical University, Jinan, Shandong 250013, China; [3]Institute of Biomedical Sciences, College of Life Sciences, Shandong Normal University, Jinan, Shandong 250014, China; [4]Department of Gynecology and Obstetrics, Tianjin Medical University General Hospital, Tianjin 300052, China

Ferroptosis is an iron-catalyzed form of regulated cell death that results from the accumulation of lipid peroxidation products and reactive oxygen species to a lethal content. However, the transcriptional regulation of ferroptosis is not well understood. Sorafenib, a standard drug for hepatocellular carcinoma (HCC), induces ferroptosis in HCC cells. In this study, we conducted a CRISPR-Cas9 library screening targeting epigenetic factors and identified coactivator-associated arginine methyltransferase 1 (CARM1) as a critical inhibitor of ferroptosis. CARM1 depletion intensified Sorafenib-induced ferroptosis, resulting in decreased cell viability, reduced cellular glutathione level, increased lipid peroxidation, and altered mitochondrial crista structure. Additionally, we investigated a CARM1 inhibitor (CARM1i) as a potential ferroptosis inducer. Combining the CARM1i with Sorafenib enhanced the induction of ferroptosis. Notably, both *CARM1* knockdown and CARM1i showed cooperative effects with Sorafenib in inhibiting HCC growth in mice. The underlying mechanism involves CARM1-catalyzed H3R26me2a on the promoter of glutathione peroxidase 4, leading to its transcriptional activation and subsequent ferroptosis inhibition. Furthermore, Sorafenib treatment induced the transcription of CARM1 through the MDM2-p53 axis. In summary, our findings establish CARM1 as a critical ferroptosis inhibitor and highlight the potential of CARM1is as novel ferroptosis inducers, providing promising therapeutic strategies for HCC treatment.

INTRODUCTION

Ferroptosis is a recently recognized form of regulated cell death characterized by morphological changes, such as smaller mitochondria with increased mitochondrial membrane density and reduction or vanishment of mitochondrial cristae.[1] It is triggered by the accumulation of lipid peroxidation products and reactive oxygen species (ROS) resulting from dysregulated iron metabolism.[2] Pharmacological inhibitors of lipid peroxidation (e.g., ferrostatin-1 [Fer-1] and liproxstatin) and iron chelators (e.g., deferoxamine) have been identified as effective inhibitors of ferroptosis. While several genes and pathways related to iron and energy metabolism, oxidative stress, and lipid synthesis have been implicated in regulating ferroptosis sensitivity, the epigenetic regulation of this process remains largely unknown.

A major challenge in cancer treatment is selectively targeting cancer cells while sparing healthy cells. Cancer cells often exhibit defects in cell death mechanisms, such as apoptosis, which contributes to therapy resistance. Because of their increased iron requirement for growth, cancer cells are more susceptible to ferroptosis compared with normal cells.[3] The identification of U.S. Food and Drug Administration (FDA)-approved drugs as ferroptosis inducers highlights the potential of targeting ferroptosis as a promising therapeutic strategy for therapy-resistant cancers.[3] Therefore, gaining a better understanding of the underlying mechanisms regulating ferroptosis sensitivity holds promise for the development of novel cancer therapies.

Hepatocellular carcinoma (HCC) ranks as the fourth leading cause of cancer-related death worldwide.[4] Current treatment options for HCC include drug therapies and non-drug therapies, such as hepatic

Received 13 June 2023; accepted 18 October 2023;
https://doi.org/10.1016/j.omtn.2023.102063.

[5]These author contributed equally

Correspondence: Yingmei Wang, Department of Gynecology and Obstetrics, Tianjin Medical University General Hospital, Tianjin 300052, China.
E-mail: wangyingmei@tmu.edu.cn
Correspondence: Chenghao Xuan, Tianjin Key Laboratory of Female Reproductive Health and Eugenetics, Tianjin Medical University General Hospital, The Province and Ministry Co-sponsored Collaborative Innovation Center for Medical Epigenetics, Department of Biochemistry and Molecular Biology, Tianjin Medical University, Tianjin 300070, China.
E-mail: chenghaoxuan@tmu.edu.cn

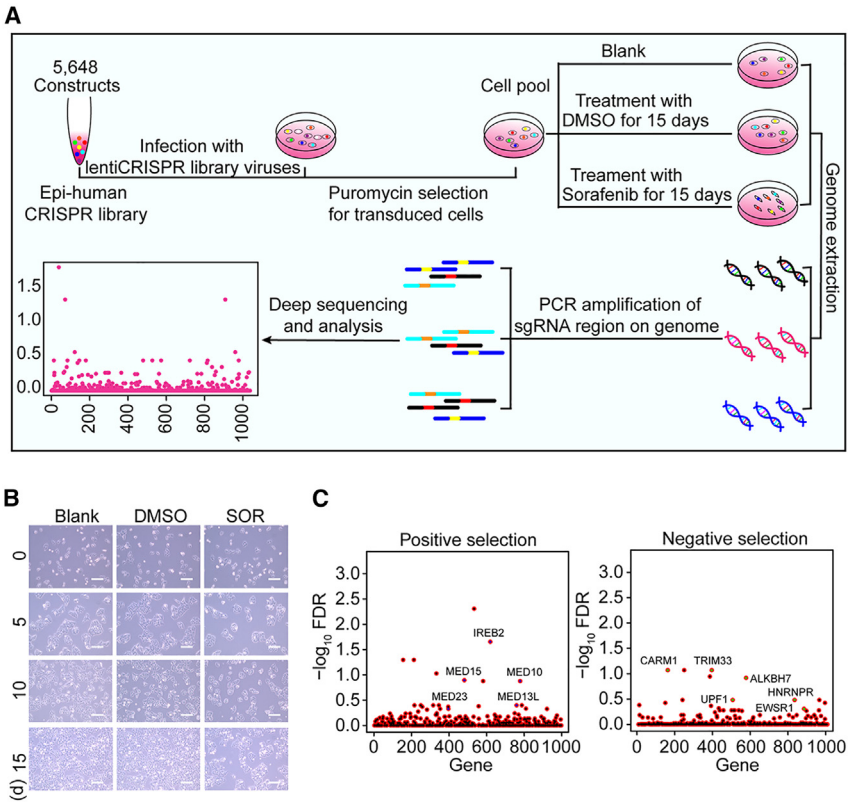

Figure 1. An epigenetic factors-targeted CRISPR-Cas9 library screening identifies CARM1 as a critical driver for Sorafenib resistance

(A) The schematic diagram presents the work flow of epigenetic factors-targeted CRISPR-Cas9 knockout library screening. Human epigenetic factors CRISPR-Cas9 knockout library containing 5,648 sgRNAs (cloned into the pLentiCRISPRv2 vector) was packed into lentiviral particle and transduced into HepG2 cells at a low multiplicity of infection. The sgRNA-transduced cells were selected by puromycin to generate a mutant cell pool. Mutant cells were treated with DMSO or 5 μM Sorafenib for 15 days for genetic screening. Genomic DNA was extracted from the treated cells and the sgRNA fragment was amplified by PCR. Copy number of sgRNAs was determined by high-throughput sequencing and analyzed by MAGeCK algorithm. (B) HepG2 cells treated with DMSO or Sorafenib, or not treated, were observed under a microscope. Scale bar, 100 μm. (C) The copy number of sgRNAs was determined by high-throughput sequencing and analyzed by the MAGeCk algorithm.

resection, liver transplantation, transarterial chemoembolization, and ablation.[4] Surgical interventions are effective for patients with early and mid-stage HCC, while small molecule targeted drugs like Sorafenib and Lenvatinib are primarily used for systemic treatment of advanced HCC.[4] Sorafenib, an FDA-approved first-line drug for unresectable HCC, exerts its antitumor effect by inhibiting various kinases, including the Ser/Thr kinase Raf, vascular endothelial growth factor receptor, and epidermal growth factor receptor.[5,6] Additionally, Sorafenib has been found to induce ferroptosis in HCC cells.[7,8] However, its efficacy is limited, suggesting the existence of primary and acquired drug resistance.[9] Hence, there is a need to develop new therapeutics to overcome Sorafenib resistance in HCC cells.

In this study, we employed a CRISPR-Cas9 knockout library targeting epigenetic factors to identify potential contributors to Sorafenib resistance in HCC cells. We identified coactivator-associated arginine methyltransferase 1 (CARM1), also known as PRMT4, as a critical driver for Sorafenib resistance in HCC. Knockdown of *CARM1* enhanced ferroptosis induced by Sorafenib and other ferroptosis inducers, while treatment with a CARM1 inhibitor (CARMi) also triggered ferroptosis in HCC cells. Notably, both *CARM1* knockdown and CARM1i exhibited cooperative effects with Sorafenib in inhibiting HCC growth in cells and mice. Mechanically, we discovered that CARM1 catalyzed the methylation of H3R26 on the promoter of glutathione peroxidase 4 (*GPX4*), leading to the transcriptional activation of *GPX4* and ferroptosis inhibition. Furthermore, we demonstrated that Sorafenib treatment induced the transcription of CARM1 through the MDM2-p53 axis. In conclusion, our findings discover a critical inhibitor of ferroptosis, providing novel strategies for treating HCC and overcoming Sorafenib resistance.

RESULTS

An epigenetic factors-targeted CRISPR-Cas9 library screening identifies CARM1 as a critical driver for Sorafenib resistance

Sorafenib, a first-line drug for HCC treatment, has been shown to induce ferroptosis in cells. However, resistance to Sorafenib is a common issue among HCC patients, limiting its effectiveness. In this study, an epigenetic factors-targeted CRISPR-Cas9 library was applied to screen epigenetic factors potentially involved in Sorafenib resistance in HCC cells. The library consisted of 5,648 single guide RNAs (sgRNAs) targeting 910 epigenetic factors, with at least 6 sgRNAs per gene, along with 131 non-targeting controls. The library was packaged into lentivirus particles and used to infect HepG2 cells to generate a cell pool. The cell pool was then treated with either DMSO, 5 μM Sorafenib, or left untreated for 15 days. After treatment, fragments containing sgRNAs were amplified by PCR and subjected to high-throughput sequencing.

In the presence of Sorafenib, cells expressing sgRNAs targeting Sorafenib resistance genes were negatively selected, resulting in a depletion of their corresponding sgRNAs in the surviving cells after 15 days of treatment. Conversely, cells carrying sgRNAs targeting Sorafenib-sensitive genes were positively selected, leading to an enrichment of their sgRNAs as determined by high-throughput sequencing (Figure 1A). During the culture of Sorafenib-resistant cells, the cell status in each group was observed under a microscope. The results demonstrated that Sorafenib treatment significantly inhibited cell viability compared

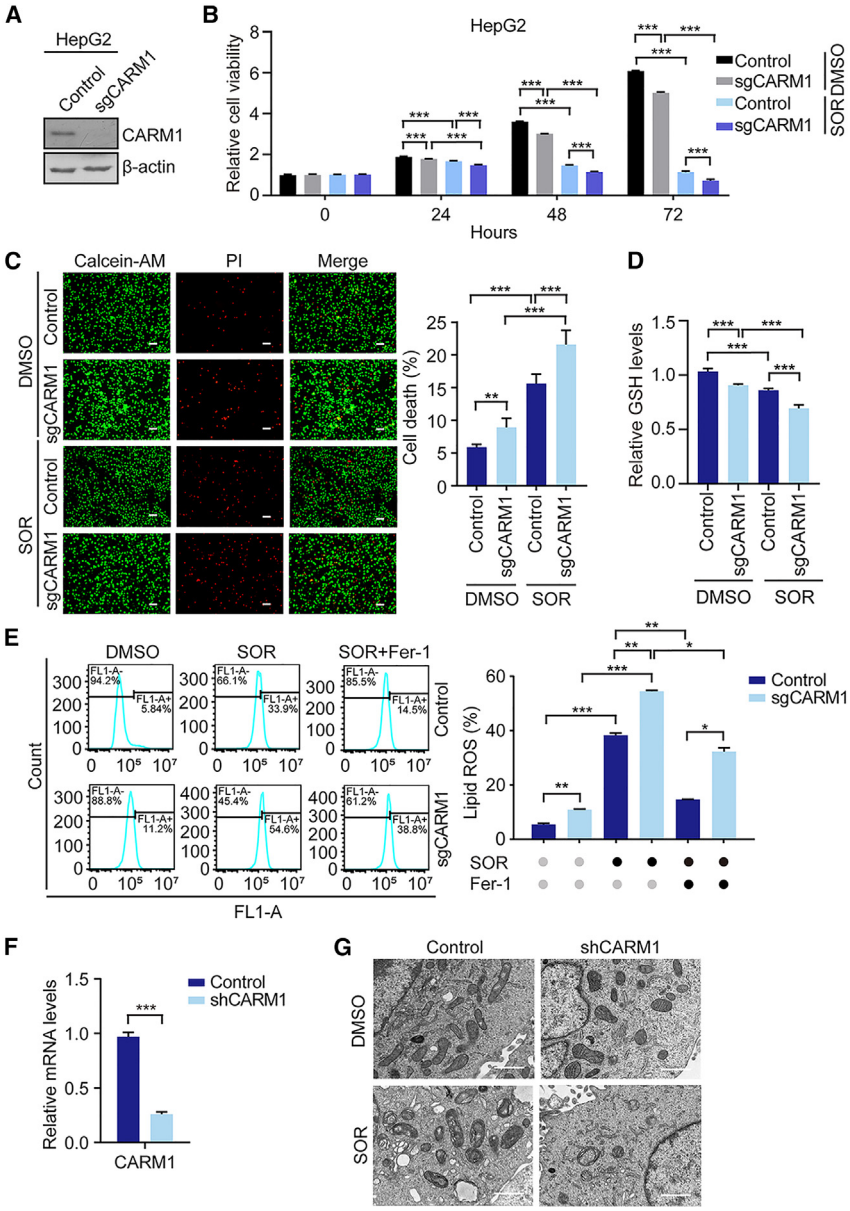

Figure 2. *CARM1* knockout/knockdown sensitizes HCC cells to Sorafenib-induced ferroptosis

(A) Cell lysate of HepG2 cells stably expressing control or *CARM1* sgRNA together with Cas9 protein was subjected to western blotting. (B) Control or *CARM1* knockout HepG2 cells were treated with DMSO or Sorafenib for indicated times, and then cell viability was examined using MTT assays. Data are mean ± SD for n = 4; ***p < 0.001 (one-way ANOVA followed by least significant difference [LSD] test for multiple comparison). (C) Control or *CARM1* knockout HepG2 cells were treated with DMSO or Sorafenib for 24 h, then stained with Calcein-AM/PI, and observed under a fluorescent microscope (left). Scale bar, 50 μm. The percentage of dead cells was calculated (right). Data are mean ± SD for n = 5; **p < 0.01, ***p < 0.001 (one-way ANOVA followed by LSD test for multiple comparison). (D) Control or *CARM1* knockout HepG2 cells were treated with DMSO or Sorafenib for 24 h, and cellular GSH was examined. Data are mean ± SD for n = 3; ***p < 0.001 (one-way ANOVA followed by LSD test for multiple comparison). (E) Control or *CARM1* knockout HepG2 cells were treated with DMSO or Sorafenib, together with or without Fer-1 (5 μM) for 24 h, and cellular lipid ROS was detected. Data are mean ± SD for n = 3; statistical significance was evaluated by one-way ANOVA followed by Tambane's T2 test for multiple comparison, *p < 0.05, **p < 0.01, ***p < 0.001. (F) The mRNAs from cells expressing control or *CARM1* shRNAs were exacted and subjected to real-time RT-PCR. Data are mean ± SD for n = 3; ***p < 0.001 (Student's t-test). (G) Control or *CARM1* knockdown HepG2 cells were treated with DMSO or Sorafenib for 24 h, and mitochondria crista was observed under a transmission electron microscope. Scale bar, 1 μm.

with the control group (Figure 1B), indicating that 5 μM Sorafenib exerted effective screening pressure in the cell culture. Our screening identified several positively selected genes, including IREB2, which has been reported to promote ferroptosis,[10] and negatively selected genes, like CARM1 (Figure 1C). Among the negatively selected genes, CARM1 ranked second. Given our previous research focused on the biological function of histone modification enzymes, we further investigated the role of CARM1 in Sorafenib resistance.

CARM1 knockout/knockdown sensitizes HCC cells to Sorafenib-induced ferroptosis

To validate the findings from our CRISPR-Cas9 knockout library screening, we generated stable *CARM1* knockout cells by infecting HCC cells with lentivirus expressing *CARM1* sgRNAs and Cas9 (Figures 2A and S1A). 3-(4, 5-dimethylthiazol-2-yl)-2, 5-diphenyl-2H-tetrazolium bromide (MTT) assays revealed that *CARM1* knockout significantly inhibited cell growth in the presence of Sorafenib (Figures 2B and S1B). To further investigate the effect of *CARM1* knockout on Sorafenib-induced cell death, calcein-AM/PI double staining assay was performed, showing that *CARM1* knockout increased the percentage of dead cells upon Sorafenib treatment (Figures 2C and S1C). Sorafenib has been reported to induce ferroptosis in HCC cells.[7,8] Therefore, we examined several markers of ferroptosis in control and *CARM1* knockout cells to determine whether *CARM1* knockout affects Sorafenib-induced ferroptosis. Our results demonstrated that *CARM1* knockout reduced cellular GSH levels (Figures 2D and S1D) and increased cellular lipid ROS levels under Sorafenib treatment (Figures 2E and S1E). Furthermore, the increased lipid ROS induced by *CARM1* knockout in the presence of Sorafenib can be rescued by the inhibitor of ferroptosis, Fer-1 (Figures 2E and S1E). Additionally, we knocked down the expression of *CARM1* using efficient short hairpin RNA (shRNA) (Figure 2F), which resulted in reduced mitochondrial cristae in HCC cells upon

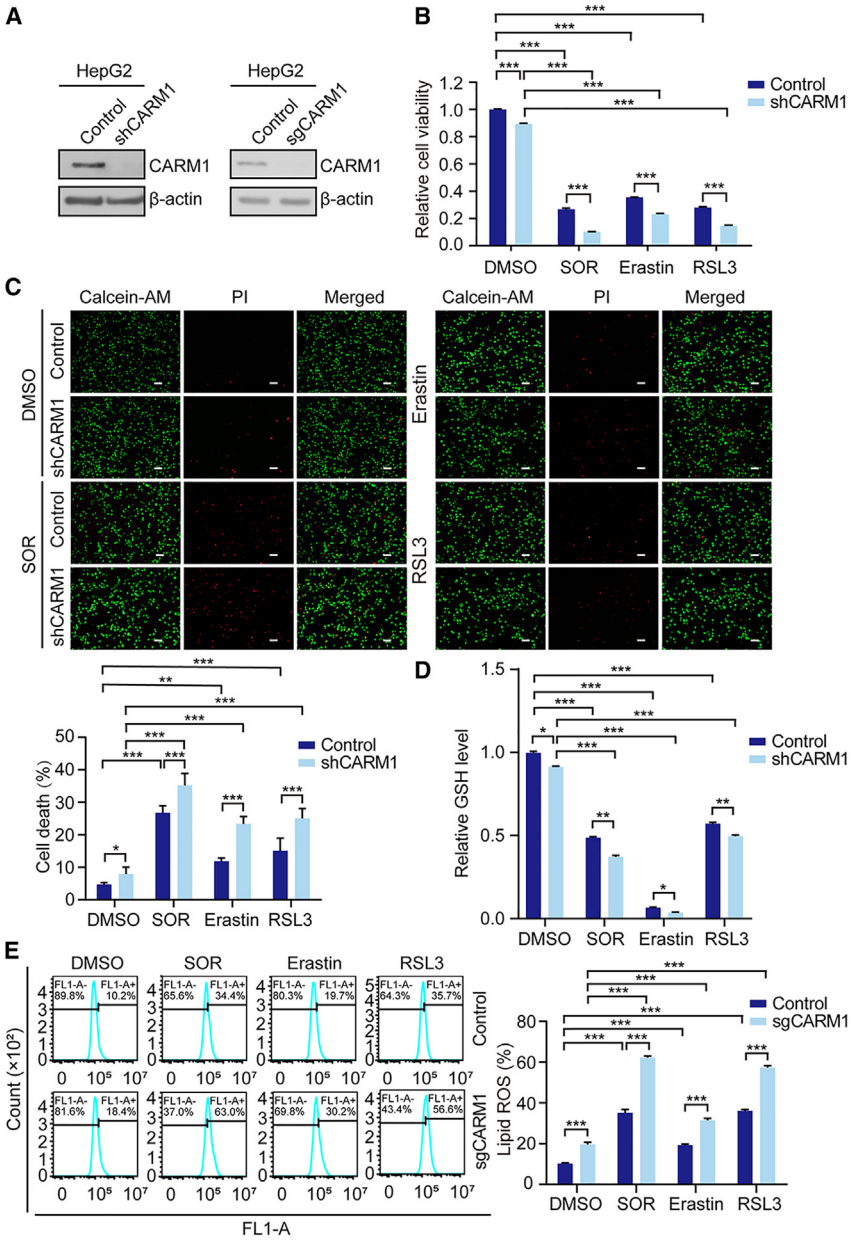

Figure 3. CARM1 negatively regulates ferroptosis in HCC cells

(A) The expression of CARM1 in control or *CARM1* knockdown/knockout HepG2 cells was detected by western blotting. (B) Control or *CARM1* knockdown HepG2 cells were treated with DMSO, Sorafenib (10 μM), Erastin (10 μM), or RSL3 (1 μM) for 72 h, and then cell viability was examined using MTT assays. Data are mean ± SD for n = 4; ***p < 0.001 (one-way ANOVA followed by Tambane's T2 test for multiple comparison). (C) Control or *CARM1* knockdown HepG2 cells were treated with DMSO, Sorafenib, Erastin, or RSL3 for 24 h, then stained with calcein-AM/PI, and observed under a fluorescent microscope (top). Scale bar, 50 μm. The percentage of dead cells was calculated (bottom). Data are mean ± SD for n = 3; *p < 0.05, **p < 0.01, ***p < 0.001 (one-way ANOVA followed by LSD test for multiple comparison). (D) Control or *CARM1* knockdown HepG2 cells were treated with DMSO, Sorafenib, Erastin, or RSL3 for 24 h, and cellular GSH was detected. Data are mean ± SD for n = 3; *p < 0.05, **p < 0.01, ***p < 0.001 (one-way ANOVA followed by Tambane's T2 test for multiple comparison). (E) Cellular lipid ROS was detected in indicated treatment group. Data are mean ± SD for n = 3; ***p < 0.001 (one-way ANOVA followed by LSD test for multiple comparison).

Sorafenib treatment (Figure 2G). Collectively, these findings demonstrate that *CARM1* knockout/knockdown promotes Sorafenib-induced ferroptosis in HCC cells.

CARM1 negatively regulates ferroptosis in HCC cells

Several small molecule compounds have been reported to induce ferroptosis. Erastin, the first discovered inducer of ferroptosis, inhibits the activity of System xc-.[1] RSL3, a GPX4 inhibitor, induces ferroptosis mainly by reducing GPX4 activity in cells.[11] To further elucidate the role of CARM1 in inhibiting ferroptosis, we treated control HCC cells, HCC cells with *CARM1* knockdown, and HCC cells with *CARM1* knockout (Figures 3A and S2A) with Sorafenib, Erastin, and RSL3, respectively. We then measured cell viability, cell death percentage, cellular GSH, and lipid ROS. Our results showed that *CARM1* knockdown/knockout enhanced ferroptosis induced by different drugs, as evidenced by decreased cell viability (Figures 3B and S2B), increased cell death percentage (Figure 3C), reduced cellular GSH levels (Figure 3D), and elevated cellular lipid ROS levels (Figure 3E) compared with control cells. Conversely, CARM1 overexpression (Figure S3A) inhibited ferroptosis induced by Sorafenib, Erastin, and RSL3, as indicated by increased cell viability (Figure S3B), decreased cell death (Figure S3C), elevated cellular GSH levels (Figure S3D), and reduced cellular lipid ROS levels (Figure S3E). These findings collectively demonstrate that CARM1 negatively regulates ferroptosis in HCC cells.

CARM1i induces ferroptosis and works cooperatively with Sorafenib to induce stronger ferroptosis in HCC cells

CARM1, a member of the arginine methyltransferase family, is known to catalyze the methylation of various proteins, including histone H3 at R16 and R27.[12,13] In our previous findings, we have demonstrated that *CARM1* knockdown/knockout sensitized HCC cells to Sorafenib-induced ferroptosis. To further investigate the involvement of CARM1's enzymatic activity in this process, we treated HCC cells with a CARM1i, a small molecule compound

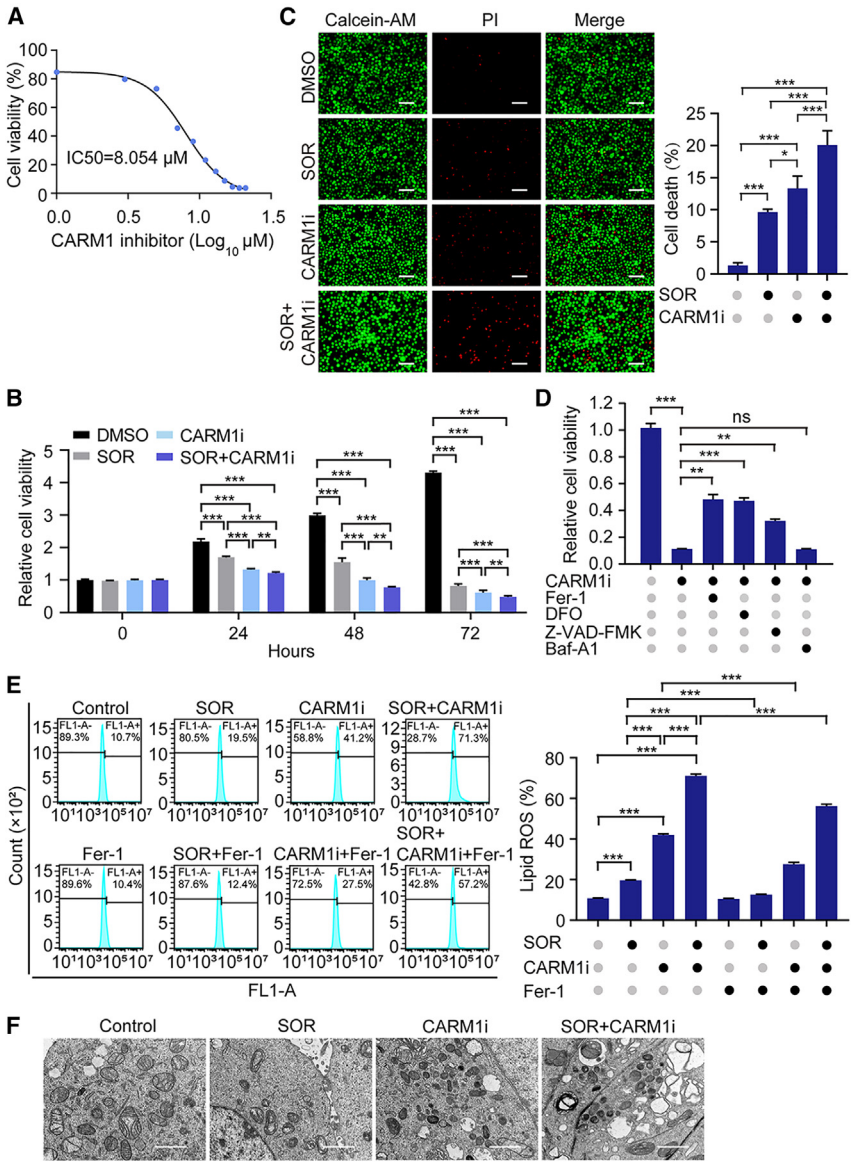

Figure 4. CARM1i can induce ferroptosis, and work cooperatively with Sorafenib to induce stronger ferroptosis in HCC cells

(A) HepG2 cells were treated with the indicated concentration of CARM1i for 24 h, and then cell viability was measured by MTT assays, and half maximal inhibitory concentration (IC_{50}) was determined. (B) HepG2 cells were treated with DMSO, Sorafenib (SOR) (10 μM), CARM1i (5 μM), and SOR (10 μM) combined with CARM1i (5 μM) for the indicated times, and then cell viability was examined using MTT assays. Data are mean ± SD for n = 4. (C) Cells treated with the indicated drug were stained with calcein-AM/PI, and observed under a fluorescent microscope. Scale bar, 50 μm. Data are mean ± SD for n = 3. (D) HepG2 cells were treated with CARM1i (5 μM) together with Fer-1 (5 μM), DFO (15 μM), Z-VAD-FMK (5 μM), or Baf-A1 (20 nM) for 72 h, and then cell viability was examined using MTT assays. Data are mean ± SD for n = 4; statistical significance was evaluated by one-way ANOVA followed by Tambane's T2 test for multiple comparison, $^{**}p < 0.01$, $^{***}p < 0.001$. ns, not significant. (E) HepG2 cells were treated with indicated drugs, and then cellular lipid ROS was detected. Data are mean ± SD for n = 3. For Figures 4B, 4C, and 4E, statistical significance was evaluated by one-way ANOVA followed by LSD test for multiple comparison, $^{*}p < 0.05$, $^{**}p < 0.01$, $^{***}p < 0.001$. (F) Mitochondria crista in HepG2 cells treated with indicated drugs was observed under a transmission electron microscope. Scale bar, 1 μm.

that targets CARM1's enzymatic function.[14] The half maximal inhibitory concentration of the CARM1i in the HepG2 cell line was determined to be 8.054 μM (Figure 4A). We found that CARM1i treatment significantly reduced the viability of HCC cells (Figure 4B) and increased cell death (Figure 4C). To determine the type of cell death induced by the CARM1i, we co-treated HepG2 cells with the CARM1i and various cell death inhibitors and assessed cell viability. Our results revealed that ferroptosis inhibitors, deferoxamine (DFO), and Fer-1, restored cell viability, while the apoptosis inhibitor, Z-VAD-FMK, only slightly increased cell viability, and the autophagy inhibitor, Baf-A1, had no effect on cell death induced by the CARM1i (Figure 4D). These findings indicate that the CARM1i specifically induces ferroptosis in HCC cells. Additionally, the CARM1i treatment significantly increased cellular lipid ROS (Figure 4E), which could be restored by Fer-1, further confirming the induction of ferroptosis by the CARM1i. Furthermore, HepG2 cells treated with 5 μM of the CARM1i for 24 h were examined using a transmission electron microscope, revealing that the mitochondria exhibited shrinkage and a decrease in the number of mitochondrial cristae, providing further evidence for the induction of ferroptosis by the CARM1i (Figure 4F).

To assess whether CARM1i and Sorafenib can cooperatively induce ferroptosis in HCC cells, we combined 10 μM Sorafenib with 5 μM CARM1i to treat HCC cells. Cell viability, cell death, cellular lipid ROS levels, and mitochondrial cristae were examined, all of which demonstrated a more pronounced ferroptotic effect (Figures 4B, 4C, 4E, and 4F). It is worth noting that the proportion of ferroptosis induced by CARM1i was higher than that induced by Sorafenib alone (Figures 4B, 4C, 4E, and 4F), suggesting that the CARM1i can be used as an effective ferroptosis inducer in HCC cells.

CARM1 knockdown/inhibition sensitizes HCC to Sorafenib treatment in mice

We have demonstrated that CARM1 depletion/inhibition promotes the sensitivity of HCC cells to Sorafenib-induced ferroptosis by *in vitro*

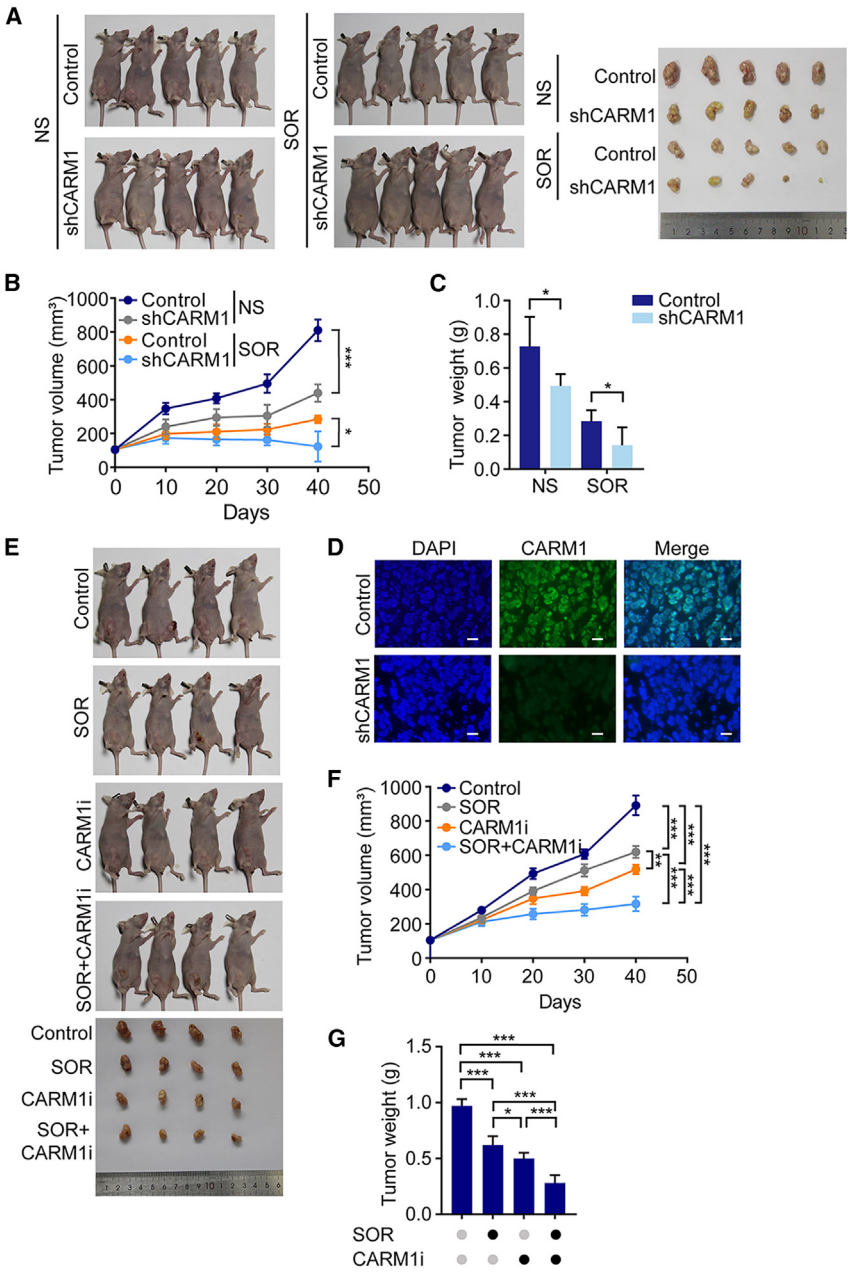

Figure 5. CARM1 knockdown/inhibition sensitizes HCC to Sorafenib treatment in mice

(A) HepG2 cells stably expressing control or *CARM1* shRNAs were transplanted into female athymic nude mice. When the tumor volume reached 100 mm^3, mice were administered by gavage with vehicle (normal saline [NS]) or Sorafenib (SOR) (20 mg/kg/day). Tumors were stripped out 40 days later and photographed. (B) Tumors were measured every 10 days after drug treatment using a Vernier caliper and the volume was calculated according to the formula: $V = \pi/6 \times \text{length} \times \text{width}^2$. Each bar represents the mean ± SD for 5 animal measurements, *p < 0.05, ***p < 0.001 (Student's t-test). (C) The tumors were weighed. Each bar represents the mean ± SD for n = 5, *p < 0.05 (Student's t-test). (D) The tumors were stripped from mice, and the frozen sections were stained with anti-CARM1. DAPI staining was included to visualize the nuclei. Scale bar, 20 μm. (E) HepG2 cells were injected subcutaneously into the right flanks of female athymic nude mice. Indicated drug treatment was started when the subcutaneous tumor volume of nude mice reached 100 mm^3. Tumors were stripped out 40 days later and photographed. (F) Tumors were measured every 10 days after drug treatment, and the volume was calculated. (G) The tumors were weighed. For Figures 5F and 5G, each bar represents the mean ± SD for n = 4; statistical significance was evaluated by one-way ANOVA followed by LSD test for multiple comparison. *p < 0.05, **p < 0.01, ***p < 0.001.

assays. A subcutaneous tumor model in nude mice was applied to investigate the *in vivo* effect of CARM1 depletion/inhibition on HCC response to Sorafenib. Control or CARM1-depleted HepG2 cells were subcutaneously injected into nude mice. Once the tumor volume reached 100 mm^3, mice in the control and knockdown group were treated with either normal saline or Sorafenib (20 mg/kg/day) by oral gavage on a daily basis. The growth of the implanted tumors was measured every 10 days. After 40 days, the mice were euthanized, and the tumors were excised, weighed, and photographed (Figure 5A). Our results demonstrated a significant suppression of tumor growth in mice receiving *CARM1* knockdown tumors, particularly under Sorafenib treatment, as evident from the reduced tumor volume and weight in the CARM1-depleted groups (Figures 5B and 5C). The knockdown of *CARM1* expression in the xenograft was confirmed by immunofluorescent staining of CARM1 in frozen sections of the tumors (Figure 5D). These findings demonstrate that *CARM1* knockdown sensitizes HCC to Sorafenib treatment in mice.

Furthermore, we investigated whether the CARM1i could enhance the sensitivity of HCC cells to Sorafenib in nude mice. HepG2 cells were subcutaneously transplanted into nude mice. Once the tumor volume reached 100 mm^3, the mice were randomly divided into four groups: control group, Sorafenib (20 mg/kg/day) treatment group, CARM1i (1 mg/kg/day) treatment group, and Sorafenib (20 mg/kg/day) combined with CARM1i (1 mg/kg/day) treatment group. After 40 days, the mice were euthanized, and the tumors were stripped out for weighing and photographing (Figure 5E). The results showed that CARM1i significantly inhibited the growth of HCC in mice, and its therapeutic effect was superior to that of Sorafenib, even at a low dose of 1 mg/kg/day (Figures 5E–5G). Moreover, the combination of CARM1i and Sorafenib exhibited enhanced inhibition of HCC growth in mice (Figures 5E–5G). These findings collectively demonstrate that the CARM1i can effectively suppress HCC growth in mice, and the combination of CARM1i and Sorafenib has a better therapeutic effect.

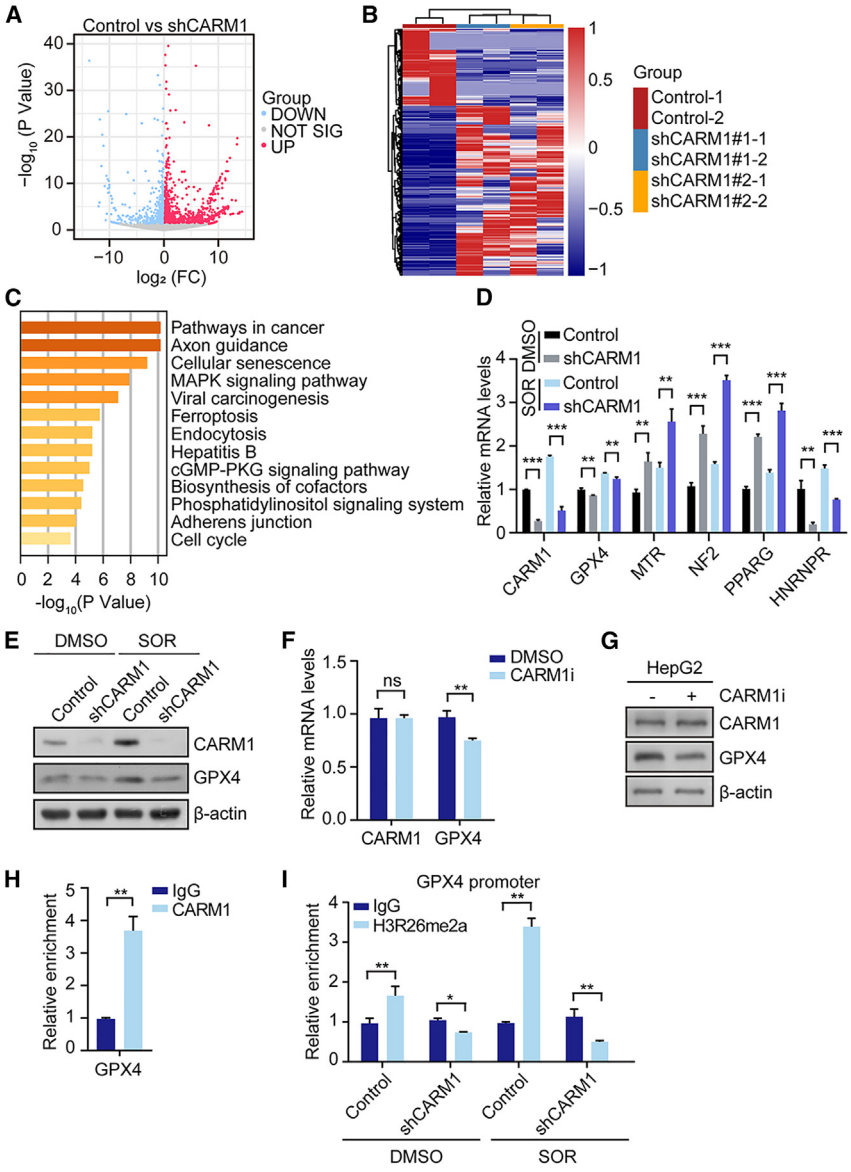

Figure 6. CARM1 transcriptionally activates *GPX4*

(A) The mRNAs from HepG2 cells expressing control shRNAs or *CARM1* shRNAs in the presence of Sorafenib (SOR) were extracted and subjected to RNA-seq. The volcano plot shows the differentially expressed genes between HepG2 cells expressing control shRNAs and *CARM1* shRNAs. At the significance of $p < 0.05$ and with |foldchange| > 1.5, significantly upregulated genes are shown as red dots and downregulated as blue dots. (B) Heatmaps show the expression of significantly dysregulated genes. (C) Kyoto Encyclopedia of Genes and Genomes enrichment analyses of significantly dysregulated genes in *CARM1* knockdown HepG2 cells. (D) Total mRNA from HepG2 cells expressing indicated shRNAs under Sorafenib treatment was extracted and quantitative real-time RT-PCR assays were performed. Each bar represents the mean ± SD for n = 3, $^{**}p < 0.01$, $^{***}p < 0.001$ vs. control (Student's t-test). (E) Western blot analysis of CARM1, GPX4, and β-actin in HepG2 cells expressing control or *CARM1* shRNAs with DMSO or Sorafenib treatment. (F) HepG2 cells were treated with DMSO or CARM1i for 24 h, and the mRNAs were extracted and quantitative real-time RT-PCR assays were performed. Each bar represents the mean ± SD for n = 3, $^{**}p < 0.01$ (Student's t-test). (G) Cell lysate of HepG2 cells treated with DMSO or CARM1i was subjected to western blotting. (H) ChIP assays were performed in HepG2 cells using CARM1 antibodies or IgG, and then real-time PCR was executed using primers targeting the promoter of *GPX4*. Each bar represents the mean ± SD for n = 3, $^{**}p < 0.01$ (Student's t-test). (I) ChIP assays were performed in HepG2 cells expressing control or *CARM1* shRNAs with or without Sorafenib treatment, using H3R26me2a antibodies or IgG, and primers targeting the promoter of *GPX4*. Each bar represents the mean ± SD for n = 3, $^{*}p < 0.05$, $^{**}p < 0.01$ (Student's t-test).

CARM1 inhibits Sorafenib-induced ferroptosis through transcriptional activation of *GPX4*

To decipher the mechanism by which *CARM1* knockdown promotes Sorafenib-induced ferroptosis, we conducted RNA sequencing (RNA-seq) analysis to identify differentially expressed transcripts in HepG2 cells with *CARM1* knockdown under Sorafenib treatment. Our bioinformatic analyses revealed that, with a significance level of $p < 0.05$, 961 genes were upregulated and 436 genes were downregulated in *CARM1* knockdown cells with |foldchange| > 1.5 (Figures 6A and 6B). Importantly, Kyoto Encyclopedia of Genes and Genomes analyses of these dysregulated genes suggested that CARM1 regulates cellular pathways related to HCC progression, such as "pathways in cancer," "cellular senescence," "[mitogen-activated protein kinase] signaling pathway," and "viral carcinogenesis" (Figure 6C). Especially, "ferroptosis" emerged as one of the most enriched biological processes (Figure 6C), further supporting the regulatory function of CARM1 in Sorafenib-induced ferroptosis. The expression alteration of several representative genes related to ferroptosis was validated in control and CARM1-depleted HepG2 cells using real-time RT-PCR assays (Figure 6D). Interestingly, the transcription of GPX4, a key inhibitor of ferroptosis, was reduced by CARM1 depletion (Figure 6D). GPX4 is the primary enzyme responsible for catalyzing the reduction of phospholipid peroxides in mammalian cells.[15,16] Western blotting results further confirmed that the protein level of GPX4 was also decreased in CARM1-depleted HepG2 cells treated with Sorafenib (Figure 6E). Based on these findings, we propose that *GPX4* may serve as a functional target gene of CARM1, contributing to Sorafenib resistance in HCC cells.

As a histone arginine methyltransferase, CARM1 activates transcription by catalyzing asymmetric dimethylation of H3R17 and H3R26 (H3R17me2a and H3R26me2a).[12,13] To determine whether the enzymatic activity of CARM1 is involved in the transcriptional regulation

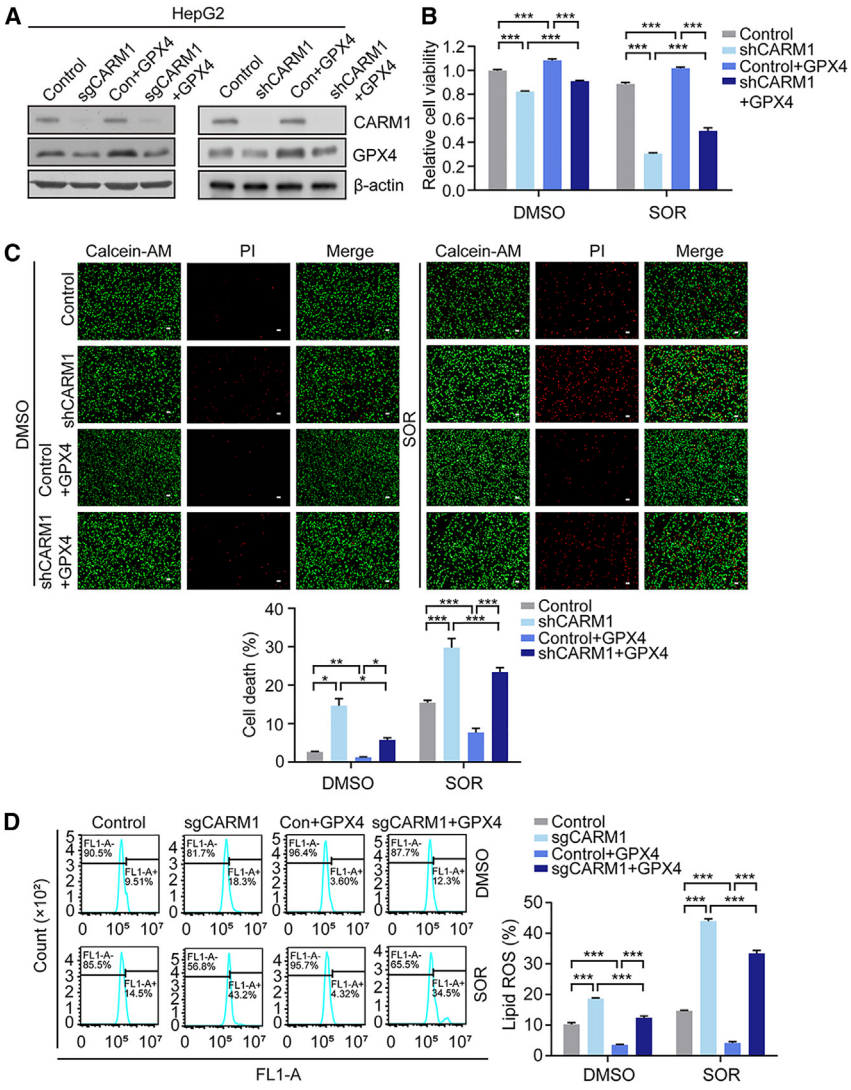

Figure 7. CARM1 inhibits Sorafenib-induced ferroptosis through transcriptional activation of *GPX4*

(A) Western blot analysis of the expression of CARM1, GPX4, and β-actin in indicated cells. (B) The viability of indicated cells was measured using MTT assays. Data are mean ± SD for n = 4; ***p < 0.001 (one-way ANOVA followed by LSD test for multiple comparisons). (C) Calcein-AM/PI staining was performed in indicated cells. Scale bar, 50 μm. Data are mean ± SD for n = 3; *p < 0.05, **p < 0.01, ***p < 0.001 (one-way ANOVA followed by LSD test or Tambane's T2 test for multiple comparisons). (D) Cellular lipid ROS was detected in indicated cells. Data are mean ± SD for n = 3; ***p < 0.001 (one-way ANOVA followed by LSD test for multiple comparison). SOR, Sorafenib.

of *GPX4*, HepG2 cells were treated with CARM1i for 24 h, and real-time RT-qPCR and western blotting were performed. The results showed that CARM1i reduced both the mRNA level (Figure 6F) and the protein level of GPX4 (Figure 6G). Additional chromatin immunoprecipitation (ChIP) assays provided evidence that CARM1 bound to the promoter region of *GPX4* (Figure 6H). To further support the hypothesis that CARM1 transcriptionally activated *GPX4* through catalyzing H3R26me2a, ChIP assays were performed in HepG2 cells stably expressing *CARM1* shRNAs or control shRNAs using H3R26me2a antibodies. The results indicated that the knockdown of *CARM1* dramatically decreased CARM1-catalyzed H3R26me2a on the promoter of *GPX4* (Figure 6I). Collectively, our data indicate that *GPX4* is a transcriptional target of CARM1 in HCC cells under Sorafenib treatment.

To prove that the downregulation of GPX4 mediates the promotion of ferroptosis caused by *CARM1* knockdown, we transfected HA-GPX4 expression constructs into *CARM1* knockdown or *CARM1* knockout cells (Figure 7A) and subsequently measured cell viability, cell death, and cellular lipid ROS. The results revealed that overexpression of GPX4 rescued the cell phenotype caused by *CARM1* knockdown/knockout, leading to the inhibition of Sorafenib-induced ferroptosis, as evidenced by increased cell viability (Figure 7B) and decreased percentages of cell death (Figure 7C) and cellular lipid ROS levels (Figure 7D) in CARM1-depleted HCC cells. Taken together, our findings demonstrate that CARM1 inhibits Sorafenib-induced ferroptosis through the transcriptional activation of *GPX4*.

Sorafenib treatment induces the transcription of *CARM1* through the MDM2-p53 axis

As shown in Figure 6E, Sorafenib treatment increased the protein level of CARM1 in HepG2 cells. To further investigate the regulation of CARM1 by Sorafenib, we analyzed the mRNA data from the GSE151412 dataset and found that Sorafenib treatment significantly increased *CARM1* mRNA levels in HCC cell lines (Hep3B and Huh7) (Figure 8A). This increase in *CARM1* mRNA levels upon Sorafenib treatment was also verified by real-time RT-PCR in HepG2 cells (Figure 8B). Previous studies have reported that p53 can bind to the promoter region of *CARM1* and inhibit its transcription.[17] Therefore, we wondered whether p53 participates in the induction of CARM1 by Sorafenib treatment in HCC cells. Western blot analysis of cell lysates from HepG2 cells treated with DMSO or Sorafenib revealed that Sorafenib treatment decreased the protein level of p53 (Figure 8C). When FLAG-p53 was overexpressed in HepG2 cells under Sorafenib treatment, the protein levels of both CARM1 and its transcriptional target GPX4 were reduced (Figure 8D). Furthermore, ChIP assays demonstrated the binding of p53 to the promoter of *CARM1*, which was significantly reduced upon Sorafenib treatment (Figure 8E). These findings

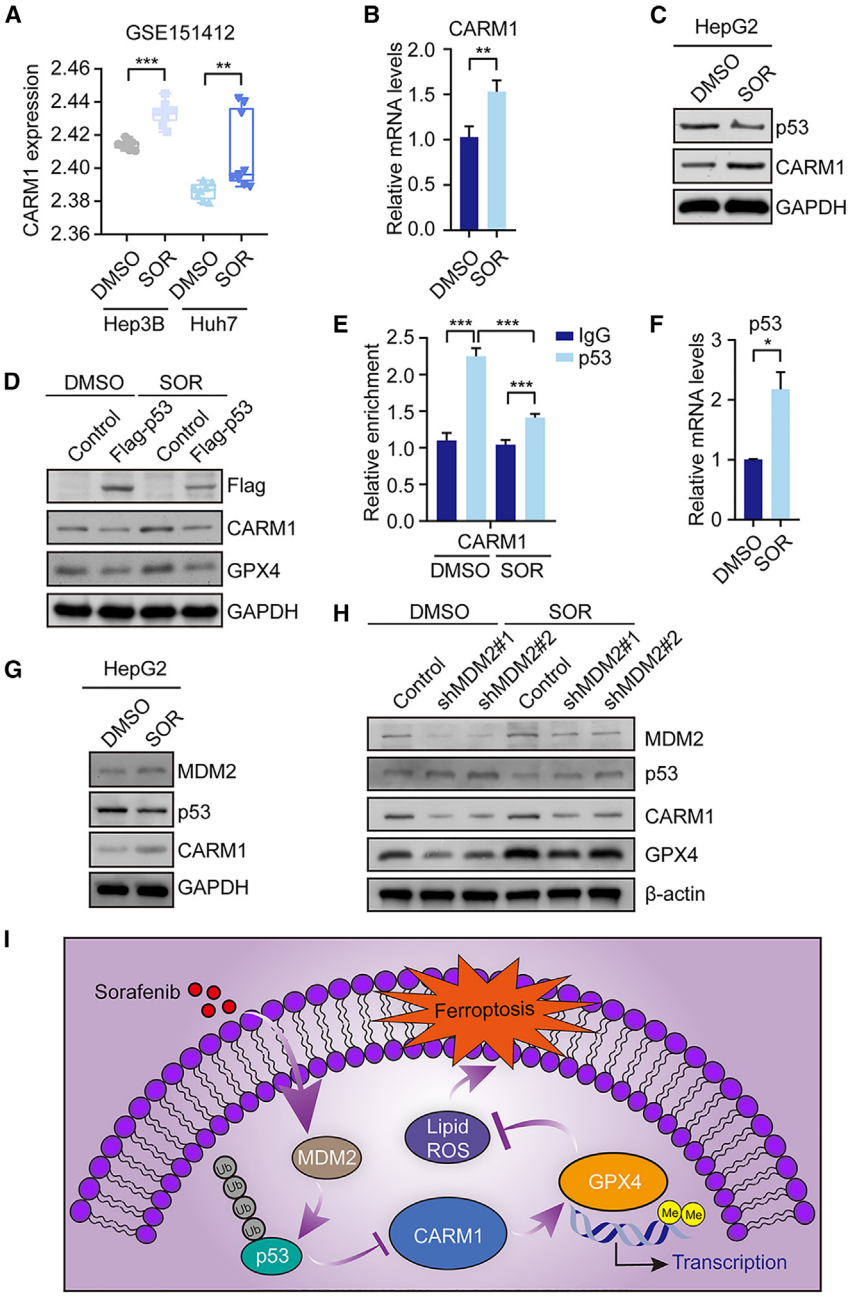

Figure 8. Sorafenib treatment induces the transcription of *CARM1* through the MDM2-P53 axis

(A) GSE151412 dataset, which includes the transcriptional data of different HCC cells treated with Sorafenib (SOR), was applied to analyze *CARM1* mRNA levels in HCC cells treated with Sorafenib or not. $^{**}p < 0.01$, $^{***}p < 0.001$ (Wilcoxon rank-sum test). (B) HepG2 cells were treated with DMSO or Sorafenib for 24 h, and the mRNAs were extracted and quantitative real-time RT-PCR assays were performed. Each bar represents the mean ± SD for n = 3, $^{**}p < 0.01$ (Student's t-test). (C) Cell lysate of HepG2 cells treated with DMSO or Sorafenib was subjected to western blotting. (D) Western blot analysis of the expression of FLAG-p53, CARM1, GPX4, and GAPDH in indicated cells. (E) ChIP assays were performed in HepG2 cells with or without Sorafenib treatment, using anti-p53 or IgG with primers targeting the promoter of *CARM1*. Each bar represents the mean ± SD for n = 3, $^{***}p < 0.01$ (one-way ANOVA followed by LSD test for multiple comparison). (F) HepG2 cells were treated with DMSO or Sorafenib for 24 h, and the mRNAs were extracted and quantitative real-time RT-PCR assays were performed. Each bar represents the mean ± SD for n = 3, $^{*}p < 0.05$ (Student's t-test). (G and H) Western blotting was performed in indicated cells. (I) The schematic figure shows the mechanism CARM1 explores to inhibit Sorafenib-induced ferroptosis in HCC cells.

collectively indicate that the depletion of p53 is responsible for the increased transcription of *CARM1* upon Sorafenib treatment.

Although the protein level of p53 was reduced by Sorafenib treatment, the mRNA level of *p53* was not decreased (Figure 8F), suggesting that the depletion of p53 caused by Sorafenib treatment is caused by the destabilization of p53 protein. MDM2 is a well known E3 ligase for p53, mediating the degradation of p53 through the ubiquitin-proteasome pathway.[18] The results of western blotting showed that the MDM2 protein level was increased by Sorafenib treatment (Figure 8G). Moreover, upon Sorafenib treatment, MDM2 knockdown led to increased p53 protein levels and decreased expression of both CARM1 and GPX4 (Figure 8H). Taken together, our findings demonstrate that Sorafenib treatment induces the expression of CARM1 through the MDM2-p53 axis, leading to the transcriptional activation of *GPX4* and subsequent inhibition of ferroptosis (Figure 8I), providing insights into the possible mechanism of Sorafenib resistance in HCC cells.

DISCUSSION

Ferroptosis is regulated form of cell death that occurs through excessive peroxidation of polyunsaturated fatty acid-containing phospholipids, and several genes related to iron or energy metabolism, lipid synthesis, and oxidative stress have been identified as regulators of ferroptosis.[1] For example, inhibiting lysosomal activity or silencing nuclear receptor coactivator 4, which recruits ferritin to autophagosomes for lysosomal degradation and iron release, can suppress ferroptosis.[19,20] Depleting acyl-coenzyme A synthetase long-chain family member 4, or knocking down lysophosphatidylcholine acyltransferase 3, which are involved in the metabolism of polyunsaturated fatty acids, also inhibits ferroptosis.[21–23] Other regulators of ferroptosis include enzymes in the mevalonate pathway, such as farnesyldiphosphate farnesyltransferase 1,[24] cysteinyl-tRNA synthetase in the trans-sulfuration pathway, glutaminolysis,[25] and Fanconi anemia complementation group D2.[26]

However, studies on the transcriptional regulation of ferroptosis are scarce. In our study, we used a CRISPR-Cas9 library to screen for epigenetic factors potentially involved in Sorafenib-induced ferroptosis in HCC cells, and identified CARM1 as a driver gene for Sorafenib resistance. We further demonstrated that CARM1 negatively regulates ferroptosis in HCC cells by transcriptionally activating *GPX4*, a major protective enzyme against peroxidation damage. Our findings provide a theoretical basis for understanding the transcriptional regulation of ferroptosis.

The canonical pathway for inducing ferroptosis involves inactivating GPX4, which is responsible for removing hydroperoxides in phospholipids and cholesterol, even when they are inserted into membranes or lipoproteins.[27] GPX4 can be inactivated through the depletion of intracellular GSH or by binding of compounds to its active sites. In some cells, direct inhibition of GSH synthesis, such as through the use of buthionine sulfoximine, can induce ferroptosis.[28] Additionally, compounds like RSL3, ML162, withaferin A, and altretamine can induce ferroptosis by inactivating GPX4.[28–31] In our study, we discovered that inhibiting CARM1 activity transcriptionally inhibits *GPX4*, making CARM1i a novel ferroptosis inducer. Notably, the CARM1i showed better efficacy in inducing ferroptosis and suppressing HCC growth in mice than Sorafenib, even at a lower dose. Furthermore, *CARM1* and *GPX4* exhibited higher expression levels in LIHC tissues compared with normal tissues (Figure S4A), and the Kaplan-Meier survival analysis revealed a significant association between high expression of *CARM1* and *GPX4* and poor prognosis (Figure S4B). Therefore, using CARM1i alone or a combination of CARM1i and Sorafenib may offer new therapeutic strategies for HCC.

In addition, p53, as the guardian of the genome, functions as a crucial tumor suppressor through inducing cell-cycle arrest, senescence, or apoptosis.[32] p53 also controls metabolism and redox state, contributing to preventing or promoting ferroptosis, depending on the cellular context, especially the ROS stress level.[33,34] In our study, we discovered a novel mechanism p53 explores to regulate ferroptosis. We showed that, in response to Sorafenib treatment, the stress response within cells led to MDM2-catalyzed degradation of p53, relieved p53-mediated transcriptional inhibition of *CARM1*, and subsequently resulted in ferroptosis suppression.

In summary, we identified CARM1 as a key inhibitor of ferroptosis in HCC cells, and discovered CARM1i as a novel ferroptosis inducer. Targeting CARM1 may be a potential therapeutic strategy for treating HCC or overcoming Sorafenib resistance.

MATERIALS AND METHODS

Cells and reagents

HepG2 and Hep3B cells were cultured in DMEM supplemented with 10% fetal bovine serum (FBS) (Biological Industries, Beit HaEmek, Israel) at 37°C in a humidified atmosphere with 5% CO_2. Cell lines were authenticated by examining their morphology and growth characteristics. All cells were regularly tested using the mycoplasma detection kit (D101, Vazamy, Nanjing, China). Anti-GPX4 (ab125066), anti-MDM2 (ab16895) and anti-H3 (asymmetric di methyl R26) (ab194679) were purchased from Abcam Inc. (Cambridge, MA). Anti-β-actin (AC026) was bought from Abclonal Technology Co. (Wuhan, Hubei, CN). Anti-Ki67 (D2H10), anti-GAPDH (2118), and anti-CARM1 (12495) were purchased from Cell Signaling Technology (Danvers, MA). Anti-p53 (sc-126) was purchased from Santa Cruz Biotechnology Inc. (Dallas, TX), and anti-FLAG (M2, F3165) was purchased from Merck KGaA (Darmstadt, Germany). Horseradish peroxidase-conjugated secondary antibodies (5220-0341 and 5220-0336) were purchased from SeraCare Co. (Milford, MA). Sorafenib (HY-10201, final concentration 10 μM), erastin (HY-15763, final concentration 10 μM), RSL3 (HY-100218A, final concentration 1 μM), DFO (HY-D0903, final concentration 15 μM), Z-VAD-FMK (HY-16658B, final concentration 5 μM) were purchased from MedChemExpress (Monmmouth Junction, NJ). Fer-1 (T6500, final concentration 5 μM) was purchased from Target Molecule Co. (Boston, MA). CARM1i (217531, final concentration 5 μM), bafilomycin A1 (Baf-A1, 196000, final concentration 20 nM) were purchased from Merck KGaA.

An epigenetic factors-targeted CRISPR-Cas9 knockout library screen

To identify epigenetic factors involved in Sorafenib resistance in HepG2 cells, the human epigenetic factors CRISPR-Cas9 knockout library was adopted. The library containing 5,648 sgRNAs (cloned into the pLentiCRISPRv2 vector) targeting 910 epigenetic factors (at least 6 sgRNAs per gene and 131 non-targeting controls) was a gift from Fei Lan (Fudan University, China). The library plasmids were transfected into HEK293T cells along with packaging plasmids psPAX2 and pMD2.G to generate a lentivirus particle pool. Then this lentivirus pool was transduced into HepG2 cells at a low multiplicity of infection (about 0.3). The transduced cells were selected with puromycin (1 μg/mL) for 7 days to generate a mutant cell pool. The mutant cells were treated with DMSO (2 biological replications) or 5 μM Sorafenib (2 biological replications), or not treated respectively for 15 days. Then, at least 1×10^8 cells in each group were collected for the extraction of genomic DNA. The sgRNA fragments were amplified by PCR using Platinum II Hot-Start Green PCR Master Mix 2X (14001012), which was purchased from Thermo Fisher Scientific Inc. (Waltham, MA), and primers (CRISPR V2 F: 5′-CTTG TGGAAAGGACGAAACACCG-3′, CRISPR V2 R: 5′-CGACTCG GTGCCACTTTTTCA-3′). Finally, high-throughput sequencing was carried out by BGI Genomics Co., Ltd (Beijing, China), and the sgRNA read count was analyzed by the MAGeCk algorithm.

Gene expression knockdown and gene knockout

Efficient siRNA sequences such as siMDM2-1 (5′-GATTCCAGA GAGTCATGTGTT-3′), and siMDM2-2 (5′-CGATTATATGATGA GAAGCAA-3′) were cloned into pLKO.1 lentivirus shRNA vector to achieve shRNA-mediated silencing. The PLKO-shCARM1-1 and PLKO-shCARM1-2 plasmids were gifts from Xudong Wu at Tianjin Medical University. These lentiviral constructs were co-transfected into HEK293T cells with packaging vectors psPAX2 and pMD2.G using PEI (40815ES03, Yeason Biotechnology, Shanghai, China) to

generate lentivirus expressing shRNAs. For sgRNA-mediated *CARM1* knockout, sgRNA sequences (ATCCAGTTCGCCAC ACCCAA) were cloned into the pLentiCRISPRv2 vector. This lentiviral construct was co-transfected into HEK293T cells with packaging vectors psPAX2 and pMD2.G to produce lentivirus expressing *CARM1* sgRNA and Cas9 protein.

Cell viability assays

Cell viability was determined using the MTT assay. In brief, 2,500 cells suspended in 100 μL DMEM with 10% FBS were seeded into a well of a 96-well plate. Twenty-four hours later, the cells were incubated in the presence of DMSO or other drugs for 24, 48, or 72 h. Then, an MTT solution (final concentration is 0.5 mg/mL) prepared in DMEM was applied to replace the medium. After incubation for 4 h at 37°C, the medium was discarded, and cells were lysed for 30 min at room temperature with DMSO. The absorbance was measured at 490 nm by a spectrophotometer.

Calcein-AM/PI double staining

About 1×10^5 HepG2 cells were placed in a 6-cm dish. After treatment with indicated drugs for 24 h, the cells were digested by trypsin, collected, and washed twice with PBS buffer. Then the cells were stained using Calcein-AM/PI double staining kit (C542, Dojindo Molecular Technologies, Inc, Kumamoto Ken, Japan). The green fluorescence-labeled living cells and red fluorescence-labeled dead cells were observed simultaneously under a fluorescence microscope, and the proportion of dead and living cells was calculated.

Reduced GSH measurement

About 2×10^6 HepG2 cells were placed in a 10-cm dish. Twenty-four hours later, cells were treated with indicated drugs for 24 h. Cells were collected and counted. The content of reduced glutathione was determined by Reduced GSH Assay kit (BC1175, Solarbio Life Science, Beijing, China) according to the manufacturer's instructions.

Lipid peroxidation measurement

About 1×10^5 HepG2 cells were placed in a 6-cm dish. After treatment with the indicated drugs for 24 h, the cells were digested by trypsin, collected, and washed twice with PBS. The cell pellet was suspended with BODIPY 581/591 C11 with final concentration 5 μM (D3861, Thermo Fisher Scientific Inc.), and incubated at 37°C for 30 min in the dark. The cells were washed twice with PBS to remove excess BODIPY 581/591 C11, and re-suspended in 500 μL PBS. The level of lipid peroxidation was determined by a flow cytometer (Becton Dickinson, Frankin Lakes, NJ).

RNA-seq and data analyses

HepG2 cells stably expressing control shRNA, shCARM1-1, or shCARM1-2 were treated with Sorafenib for 24 h, and lysed using Trizol reagent. The mRNA was extracted from each sample and subjected to RNA-seq by Annoroad Gene Technology (Beijing, China). Following high-throughput sequencing, reads containing adapters, poly-N and low-quality sequences were removed by Annoroad Gene Technology. Trimmed reads were mapped to the human reference genome (UCSC hg38) using Hisat2 (v2.2.1), and then transcripts were assembled using StringTie (v2.2.1). Gene expression levels were quantified as gene counts using the PrepDE.py script. DESeq2 was used to perform differential gene expression analyses between samples.

ChIP

Cells were rinsed twice with PBS, and then cross-linked with 15 mL 1% formaldehyde solution for 10 min at room temperature. Then the cells were quenched with 1 mL 2 M glycine (final concentration, 0.125 M), and rinsed twice with PBS. The cells were harvested in SDS buffer (100 mM NaCl, 50 mM Tris-HCl, pH 8.1, 5 mM EDTA, and 10% SDS) containing protease inhibitors (B14002, Bimake, Houston, TX), and spun for 6 min at 1,200 rpm. Cell pellets were resuspended in ice-cold IP buffer (100 mM NaCl, 66.67 mM Tris-HCl, pH 8.0, 5 mM EDTA, 0.33% SDS, and 1.67% Triton X-100) and sonicated by Bioruptor (Diagenode, Liege, Belgium). After centrifugation at 13,000 rpm for 15 min at 4°C, H3R26me2a, CARM1, or p53 antibodies were added to the supernatant for rotation overnight in a cold room. Protein A/G beads (B23201, Bimake) were then added for another 2 h at 4°C. Beads were rinsed three times with washing buffer 1 (1% Triton X-100, 0.1% SDS, 150 mM NaCl, 2 mM EDTA, and 20 mM Tris-HCl, pH 8.0), and once with washing buffer 2 (1% Triton X-100, 0.1% SDS, 500 mM NaCl, 2 mM EDTA, and 20 mM Tris-HCl, pH 8.0), followed by reverse crosslinking in de-cross-linking buffer (1% SDS, 0.1M $NaHCO_3$) for 4 h at 65°C. The DNA was then extracted and subjected to quantitative PCR. The ChIP primers:

GPX4-ChIP-F: 5′-AGCCGGATAACTGCGCTGCCTC-3′;

GPX4-ChIP-R: 5′-GGACGCGCGTCGGCTTTCCGCG-3′;

CARM1-ChIP-qPCR-F: 5′-TGCGGAGCCTCCTGG-3′;

CARM1-ChIP-qPCR-R: 5′-TGTGAGCCACTGCGAGG-3′.

Immunohistochemistry analysis

In brief, transplanted tumors from mice were immersed in O.C.T. compound (#4583, SAKURA, Torrance, CA, USA) and solidified at −40°C. Then, the embedded specimens were sliced into 8-μm serial sections and stored at −80°C before further processing. The slices were treated with 3% hydrogen peroxide in dark for 10 min to quench endogenous peroxidases, and then blocked in PBS with 0.1% Triton X-100 (PBST) containing 10% goat serum for 1 h. The slices were incubated with primary antibodies diluted in 10% goat serum in PBST overnight at 4°C. After rinsing three times with PBST, the sections were incubated with a biotinylated secondary antibody at RT for another 1 h, and then incubated with DAB substrate solution for 5–10 s and counterstained with hematoxylin. Finally, the sections were dehydrated, mounted on coverslips, and observed under a microscope.

Animal experiments

We collected 1×10^6 HepG2 cells stably expressing efficient shRNAs targeting *CARM1* or control shRNAs and suspended them in 50 μL

PBS, which were then mixed with 50 μL Matrigel and injected subcutaneously into the right flanks of female athymic nude mice (BALB/c, Charles River Laboratories, Wilmington, MA; 5–6 weeks of age; 6 mice per group). When the tumor volume reached 100 mm^3, mice were administered by gavage with vehicle (physiological saline) or Sorafenib (20 mg/kg/day). To assess the effect of the combination of Sorafenib and CARMi treatment on HCC growth *in vivo*, 1×10^6 HepG2 cells suspended in 50 μL PBS were mixed with 50 μL Matrigel and injected subcutaneously into the right flanks of female athymic nude mice. Drug treatment started when the subcutaneous tumor volume of nude mice reached 100 mm^3. The mice were divided into four groups: (1) treated with physiological saline by gavage and with DMSO by intraperitoneal injection every day; (2) treated with Sorafenib (20 mg/kg/day) by gavage and with DMSO by intraperitoneal injection every day; (3) treated with physiological saline by gavage and with CARMi (1 mg/kg/day) by intraperitoneal injection every day; and (4) treated with Sorafenib (20 mg/kg/day) by gavage and with CARMi (1 mg/kg/day) by intraperitoneal injection every day. Tumor volume was measured every 10 days using a Vernier caliper and calculated according to the following formula: $V = \pi/6 \times \text{length} \times \text{width}^2$. The mice were sacrificed 40 days later. Tumors were then isolated and photographed. Animal handling and procedures were approved by the Institutional Animal Care and Use Committees of Tianjin Medical University.

Statistical analysis

Statistical analysis was performed using SPSS and excel softwares. All results are presented as mean ± SD, and $p < 0.05$ indicates statistical significance.

DATA AND CODE AVAILABILITY

The raw and processed high-throughput RNA-seq data were deposited in the Gene Expression Omnibus (GEO) database under accession number GSE215263. The raw and processed high-throughput sequencing data of sgRNA fragments from the epigenetic factors-targeted CRISPR-Cas9 knockout library screening were deposited in the GEO database under accession number GSE215909.

SUPPLEMENTAL INFORMATION

Supplemental information can be found online at https://doi.org/10.1016/j.omtn.2023.102063.

ACKNOWLEDGMENTS

This work was supported by the National Natural Science Foundation of China (32070647 and 32270861 to C.X.), and Key Projects of Tianjin Applied Basic Research Diversified Investment Foundation (21JCZDJC01020 to C.X.).

AUTHOR CONTRIBUTIONS

C.X. conceived the project and wrote the manuscript; C.X., Y.C., and X.W. designed the experiments; Y.C. and X.W. performed most of the experiments; Y.W. and X.L. analyzed the GEO data, TCGA data, and RNA-seq data; L.Z., B.L., H.C., Z.L., Y.S., L.X., S.F., Y.G., and S.H. performed some experiments; J.Z. and Y.W. revised the manuscript.

DECLARATION OF INTERESTS

Authors declare that they have no competing interests.

REFERENCES

1. Dixon, S.J., Lemberg, K.M., Lamprecht, M.R., Skouta, R., Zaitsev, E.M., Gleason, C.E., Patel, D.N., Bauer, A.J., Cantley, A.M., Yang, W.S., et al. (2012). Ferroptosis: an iron-dependent form of nonapoptotic cell death. Cell *149*, 1060–1072.
2. Xie, Y., Hou, W., Song, X., Yu, Y., Huang, J., Sun, X., Kang, R., and Tang, D. (2016). Ferroptosis: process and function. Cell Death Differ. *23*, 369–379.
3. Hassannia, B., Vandenabeele, P., and Vanden Berghe, T. (2019). Targeting Ferroptosis to Iron Out Cancer. Cancer Cell *35*, 830–849.
4. Chen, Z., Xie, H., Hu, M., Huang, T., Hu, Y., Sang, N., and Zhao, Y. (2020). Recent progress in treatment of hepatocellular carcinoma. Am. J. Cancer Res. *10*, 2993–3036.
5. Llovet, J.M., Ricci, S., Mazzaferro, V., Hilgard, P., Gane, E., Blanc, J.F., de Oliveira, A.C., Santoro, A., Raoul, J.L., Forner, A., et al. (2008). Sorafenib in advanced hepatocellular carcinoma. N. Engl. J. Med. *359*, 378–390.
6. Liu, Z., Lin, Y., Zhang, J., Zhang, Y., Li, Y., Liu, Z., Li, Q., Luo, M., Liang, R., and Ye, J. (2019). Molecular targeted and immune checkpoint therapy for advanced hepatocellular carcinoma. J. Exp. Clin. Cancer Res. *38*, 447.
7. Sun, X., Niu, X., Chen, R., He, W., Chen, D., Kang, R., and Tang, D. (2016). Metallothionein-1G facilitates sorafenib resistance through inhibition of ferroptosis. Hepatology *64*, 488–500.
8. Sun, X., Ou, Z., Chen, R., Niu, X., Chen, D., Kang, R., and Tang, D. (2016). Activation of the p62-Keap1-NRF2 pathway protects against ferroptosis in hepatocellular carcinoma cells. Hepatology *63*, 173–184.
9. Zhai, B., and Sun, X.Y. (2013). Mechanisms of resistance to sorafenib and the corresponding strategies in hepatocellular carcinoma. World J. Hepatol. *5*, 345–352.
10. Zhu, T., Xiao, Z., Yuan, H., Tian, H., Chen, T., Chen, Q., Chen, M., Yang, J., Zhou, Q., Guo, W., et al. (2022). ACO1 and IREB2 downregulation confer poor prognosis and correlate with autophagy-related ferroptosis and immune infiltration in KIRC. Front. Oncol. *12*, 929838.
11. Sui, X., Zhang, R., Liu, S., Duan, T., Zhai, L., Zhang, M., Han, X., Xiang, Y., Huang, X., Lin, H., and Xie, T. (2018). RSL3 Drives Ferroptosis Through GPX4 Inactivation and ROS Production in Colorectal Cancer. Front. Pharmacol. *9*, 1371.
12. Chen, D., Ma, H., Hong, H., Koh, S.S., Huang, S.-M., Schurter, B.T., Aswad, D.W., and Stallcup, M.R. (1999). Regulation of transcription by a protein methyltransferase. Science *284*, 2174–2177.
13. Schurter, B.T., Koh, S.S., Chen, D., Bunick, G.J., Harp, J.M., Hanson, B.L., Henschen-Edman, A., Mackay, D.R., Stallcup, M.R., and Aswad, D.W. (2001). Methylation of histone H3 by coactivator-associated arginine methyltransferase 1. Biochemistry *40*, 5747–5756.
14. Cheng, D., Valente, S., Castellano, S., Sbardella, G., Di Santo, R., Costi, R., Bedford, M.T., and Mai, A. (2011). Novel 3, 5-bis (bromohydroxybenzylidene) piperidin-4-ones as coactivator-associated arginine methyltransferase 1 inhibitors: enzyme selectivity and cellular activity. J. Med. Chem. *54*, 4928–4932.
15. Ursini, F., Maiorino, M., Valente, M., Ferri, L., Gregolin, C., and Metabolism, L. (1982). Purification from pig liver of a protein which protects liposomes and biomembranes from peroxidative degradation and exhibits glutathione peroxidase activity on phosphatidylcholine hydroperoxides. Biochim. Biophys. Acta *710*, 197–211.
16. Maiorino, M., Conrad, M., and Ursini, F. (2018). GPx4, lipid peroxidation, and cell death: discoveries, rediscoveries, and open issues. Antioxidants Redox Signal. *29*, 61–74.
17. Behera, A.K., Bhattacharya, A., Vasudevan, M., and Kundu, T.K. (2018). p53 mediated regulation of coactivator associated arginine methyltransferase 1 (CARM1) expression is critical for suppression of adipogenesis. FEBS J. *285*, 1730–1744.
18. Honda, R., Tanaka, H., and Yasuda, H. (1997). Oncoprotein MDM2 is a ubiquitin ligase E3 for tumor suppressor p53. FEBS Lett. *420*, 25–27.
19. Torii, S., Shintoku, R., Kubota, C., Yaegashi, M., Torii, R., Sasaki, M., Suzuki, T., Mori, M., Yoshimoto, Y., Takeuchi, T., and Yamada, K. (2016). An essential role for functional lysosomes in ferroptosis of cancer cells. Biochem. J. *473*, 769–777.

20. Gao, M., Monian, P., Pan, Q., Zhang, W., Xiang, J., and Jiang, X. (2016). Ferroptosis is an autophagic cell death process. Cell Res. *26*, 1021–1032.

21. Dixon, S.J., Winter, G.E., Musavi, L.S., Lee, E.D., Snijder, B., Rebsamen, M., Superti-Furga, G., and Stockwell, B.R. (2015). Human Haploid Cell Genetics Reveals Roles for Lipid Metabolism Genes in Nonapoptotic Cell Death. ACS Chem. Biol. *10*, 1604–1609.

22. Doll, S., Proneth, B., Tyurina, Y.Y., Panzilius, E., Kobayashi, S., Ingold, I., Irmler, M., Beckers, J., Aichler, M., Walch, A., et al. (2017). ACSL4 dictates ferroptosis sensitivity by shaping cellular lipid composition. Nat. Chem. Biol. *13*, 91–98.

23. Kagan, V.E., Mao, G., Qu, F., Angeli, J.P.F., Doll, S., Croix, C.S., Dar, H.H., Liu, B., Tyurin, V.A., Ritov, V.B., et al. (2017). Oxidized arachidonic and adrenic PEs navigate cells to ferroptosis. Nat. Chem. Biol. *13*, 81–90.

24. Shimada, K., Skouta, R., Kaplan, A., Yang, W.S., Hayano, M., Dixon, S.J., Brown, L.M., Valenzuela, C.A., Wolpaw, A.J., and Stockwell, B.R. (2016). Global survey of cell death mechanisms reveals metabolic regulation of ferroptosis. Nat. Chem. Biol. *12*, 497–503.

25. Hayano, M., Yang, W.S., Corn, C.K., Pagano, N.C., and Stockwell, B.R. (2016). Loss of cysteinyl-tRNA synthetase (CARS) induces the transsulfuration pathway and inhibits ferroptosis induced by cystine deprivation. Cell Death Differ. *23*, 270–278.

26. Song, X., Xie, Y., Kang, R., Hou, W., Sun, X., Epperly, M.W., Greenberger, J.S., and Tang, D. (2016). FANCD2 protects against bone marrow injury from ferroptosis. Biochem. Biophys. Res. Commun. *480*, 443–449.

27. Brigelius-Flohé, R., and Maiorino, M. (2013). Glutathione peroxidases. Biochim. Biophys. Acta *1830*, 3289–3303.

28. Yang, W.S., SriRamaratnam, R., Welsch, M.E., Shimada, K., Skouta, R., Viswanathan, V.S., Cheah, J.H., Clemons, P.A., Shamji, A.F., Clish, C.B., et al. (2014). Regulation of ferroptotic cancer cell death by GPX4. Cell *156*, 317–331.

29. Cao, J.Y., and Dixon, S.J. (2016). Mechanisms of ferroptosis. Cell. Mol. Life Sci. *73*, 2195–2209.

30. Woo, J.H., Shimoni, Y., Yang, W.S., Subramaniam, P., Iyer, A., Nicoletti, P., Rodríguez Martínez, M., López, G., Mattioli, M., Realubit, R., et al. (2015). Elucidating Compound Mechanism of Action by Network Perturbation Analysis. Cell *162*, 441–451.

31. Weïwer, M., Bittker, J.A., Lewis, T.A., Shimada, K., Yang, W.S., MacPherson, L., Dandapani, S., Palmer, M., Stockwell, B.R., Schreiber, S.L., and Munoz, B. (2012). Development of small-molecule probes that selectively kill cells induced to express mutant RAS. Bioorg. Med. Chem. Lett. *22*, 1822–1826.

32. Bieging, K.T., Mello, S.S., and Attardi, L.D. (2014). Unravelling mechanisms of p53-mediated tumour suppression. Nat. Rev. Cancer *14*, 359–370.

33. Kaiser, A.M., and Attardi, L.D. (2018). Deconstructing networks of p53-mediated tumor suppression *in vivo*. Cell Death Differ. *25*, 93–103.

34. Kruiswijk, F., Labuschagne, C.F., and Vousden, K.H. (2015). p53 in survival, death and metabolic health: a lifeguard with a licence to kill. Nat. Rev. Mol. Cell Biol. *16*, 393–405.